The secondary nucleation of alpha-synuclein amyloid fibrils is suppressed under fully quiescent conditions

Azad Farzadfard[1,2], Thomas O. Mason[1], Antonin Kunka[1], Kaare Bjerregaard-Andersen[2], Pekka Kallunki[2] and Alexander K. Buell[1,*]

[1]*Protein Biophysics group, Department of Biotechnology and Biomedicine, Technical University of Denmark, Søltofts Plads, Building 227, 2800, Kgs. Lyngby, Denmark*

[2]*H. Lundbeck A/S, Carl Jacobsens Vej 22, 2500 København, Denmark*

*** To whom correspondence should be addressed at alebu@dtu.dk**

Abstract:

Seed amplification assays (SAAs) are a promising avenue for the early diagnosis of neurodegenerative diseases However, when amplifying fibrils from patient-derived samples in the commonly used format of multiwell plates, it is currently highly challenging to accurately quantify the aggregates. It is therefore desirable to transfer such assays into a digital format in microemulsion droplets to enable direct quantification of aggregate numbers. To achieve transfer from conventional plate-based to the microfluidic digital format, effective seed amplification needs to be achieved inside the microdroplets. It has been shown previously that alpha-synuclein fibril amplification is strongly promoted by acidic pH. Here, we establish a new set of assay conditions that enable highly efficient seed amplification in plates without any shaking. However, the same set of conditions displayed a very different behavior upon transfer to a microfluidic platform where no amplification was observed. We demonstrate that this is caused by the suppression of all secondary processes that could amplify the seeds in the complete absence of mechanical perturbations inside the microdroplets. We further show that the amplification inside droplets can be achieved by subjecting the microemulsions to high-frequency vibrations using a piezo device. Taken together, our results provide novel insights into the physical requirements of alpha-synuclein seed amplification and demonstrate a pathway towards the development of effective digital seed amplification assays.

Introduction:

Alpha-synuclein (αSyn) aggregates in the central nervous system (CNS) are a hallmark of a range of neurodegenerative diseases known as synucleinopathies including Parkinson's disease (PD), dementia with Lewy bodies (DLB), and multiple system atrophy (MSA) [1-2]. These diseases exhibit an inherently progressive nature, worsening with over time, due to their prion-like behavior [3-5]. Specifically, the spread of these aggregates into different brain regions is thought to drive the progression of the disease. Current diagnostic methods based on symptom observation and brain imaging are efficient only in the advanced stages of the disease, and are therefore unable to capture the true onset of the pathology occurring several years prior [1, 6]. Therefore, there is a critical need for improved diagnostic tools capable of early disease detection. Notably, αSyn aggregates have been detected in patient samples, e.g. cerebrospinal fluid (CSF), during the prodromal stage years before the emergence of the early motor symptoms [7-11]. However, the aggregate concentrations are very low and their detection and quantification directly from the biological samples are therefore very challenging. Various microscopic methods have been developed to detect individual aggregate particles [12-16], but their routine implementation in a clinical setting has been met with significant technical challenges.

Seed amplification assays (SAA) have emerged as a highly promising diagnostic tool for neurodegenerative diseases, showing specificity and sensitivity levels approaching 100% [17-19]. Utilizing the inherent ability of amyloid fibrils to proliferate, SAAs effectively amplify aggregates to levels detectable by conventional multiwell plate readers, utilizing the fluorescence of amyloidogenic dyes such as Thioflavin-T. This amplification occurs through cycles of fibril growth and breakage in the presence of excess of native protein [20], thereby magnifying even minute traces of aggregates present in patient samples (**Figure 1**). The amplification of the growing fibrils is induced by vigorous mechanical perturbation of the solution, such as sonication or shaking in the presence of beads. The available SAAs for αSyn show very high sensitivity towards the presence of even femtograms of aggregates in the sample (reported for pre-formed fibrils in [20], corresponding to 1.5 pM monomer equivalents in 40 µl of sample which is equivalent to a fM concentration range of aggregates, depending on their size). SAAs have achieved maximum sensitivity for prion proteins, detecting dilutions corresponding to amplification from a single aggregate [21], which define the sensitivity level that should be theoretically attainable for other amyloid proteins like αSyn. However for αSyn, conventional SAA reached its limits due to the challenges arising from *de novo* fibril formation (i.e., fibrils formed by primary nucleation), leading to false positive responses (**Figure 1, SI figure S1**). The efficient SAAs rely on a low ratio between the rate of primary nucleation (as low as possible) and secondary processes, such as fragmentation or auto-catalytic secondary nucleation to form new seeds (**Figure 1**). Aggregation kinetics dominated by secondary processes are characterized by a lag phase followed by very sharp increase of signal in the growth phase (see **supplementary figure S1** for the simulations of SAAs in different scenarios; performed using the Amylofit online server [22]). To ensure amplification occurs within a practically useful timeframe in the SAAs (hours to a few days), the secondary processes that lead to fibril proliferation must exhibit high efficiency. However at a certain point, the enhanced secondary nucleation leads to acceleration of the aggregation kinetics to a level at which it is no longer possible to distinguish between kinetic behaviors among samples with even very different initial aggregate quantities (**Supplementary figure S1**). This limits the ability of conventional SAAs to accurately quantify the aggregate concentration from patient samples.

The limitations of conventional plate-based SAAs can be circumvented with a digital assay that segregates the samples into small discrete compartments. At sufficient dilution, the small compartment size ensures that either exactly one or no aggregate is allocated into each compartment, enabling precise quantification of the original aggregate concentration by assessing the frequency of positive compartments after amplification to above the detection limit [27-29]. Moreover, compartmentalization of the reaction mixtures into water-in-oil microfluidic droplets with a PEGylated surfactant eliminates high affinity interfaces which are known to promote *de novo* aggregation of αSyn [23-24, 25-26]. The size of such water-in-oil emulsion droplets typically range from 50 to 100 µm corresponding to 65 to 524 pL volumes. These compartment volumes accommodate on average one aggregate at the aggregate concentrations of 250 and 3.18 fM, respectively, allowing for the accurate quantification of sub-femtomolar concentrations in the original test sample.

However, digital SAAs in microemulsion droplets have their own limitation. All the conventional SAAs rely on the periodic fragmentation of the elongated aggregates either by shaking of the plate in the presence or absence of beads (referred to as RT-QuIC in the literature) [10-11, 20, 30-33] or sonication of the reaction tube (referred to as PMCA in the literature) [34-36] during the experimental time course. Achieving the same level of mechanical agitation within the droplets is challenging due to their small size (and consequently low Reynolds number) and the risk of droplet merging. Consequently, alternative solution conditions, such as acidic pH can be explored in digital SAAs, which have been shown to amplify seeds via secondary nucleation without requiring agitation in multiwell plate-based SAAs[37].

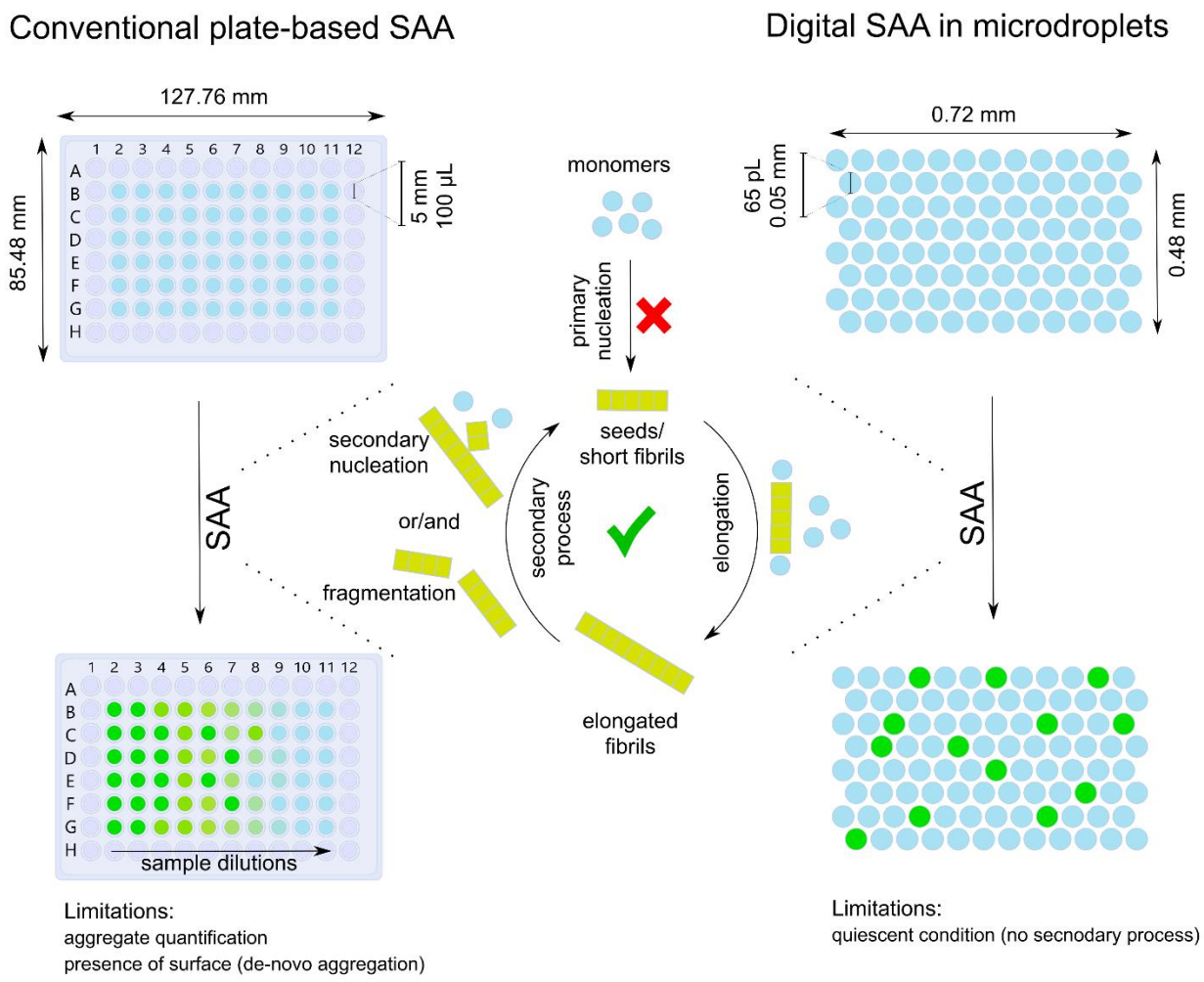

Figure 1: **Seed amplification assays in conventional multiwell-plate based (left) and digital microdroplet-based (right) setups.** The basic underlying principle of the SAA is the same for both methods (shown in the center) in which primary nucleation that increases *de novo* formation of fibrils should be suppressed and the secondary processes that increase the number of fibrils should be enhanced. Conventional plate-based SAAs suffer from false positive results due to primary nucleation in the presence of the air-water interface and a challenging quantification of added fibrils. Although the digital SAA resolves these limitations, it suffers from the difficulty of subjecting the encapsulated solutions to mechanical perturbation.

In this work, we investigate experimental conditions required for efficient αSyn seed amplification based on secondary nucleation. First, we establish a highly sensitive SAA in plates without shaking and verify its efficacy with PD brain samples. However, when conducting experiments under the same solution conditions within the microemulsion droplets, we observe no amplification of the seeds; only fibril growth occurs. We then demonstrate that even in a multiwell plate-based experiment without active shaking, gentle mechanical movements of the plate during reading cycles strongly influence the degree of amplification. Finally, we show that amplification of the seeds can also be achieved in microemulsion droplets by subjecting them to mechanical perturbations. Overall, our findings underscore that a certain degree of mechanical perturbations is essential for αSyn fibril amplification, which is otherwise not detectable under entirely quiescent conditions.

Results and discussion:

To test whether secondary nucleation was able to act as the driver of seed amplification inside water-in-oil microdroplets, we first tried to identify optimal conditions for secondary nucleation in multi-well plates. In our previous studies we had observed that mildly acidic pH (< 5.5) dramatically enhance secondary nucleation rates compared to neutral solution conditions [37]. However, the positive curvature of the aggregation growth kinetic curves as the sign of amplification was only observable in the presence of high enough amount of seeds (0.7 µM) and monomer (40 µM) during the time scale of our experiments (4 days) (**Supplementary figure S2, Supplementary table S1**). For the present study, we therefore explored a broader range of solution conditions and discovered that further lowering of the pH (final pH of ca 3) in the presence of 250 mM Na_2SO_4 leads to highly efficient seed amplification (**Figure 2**).

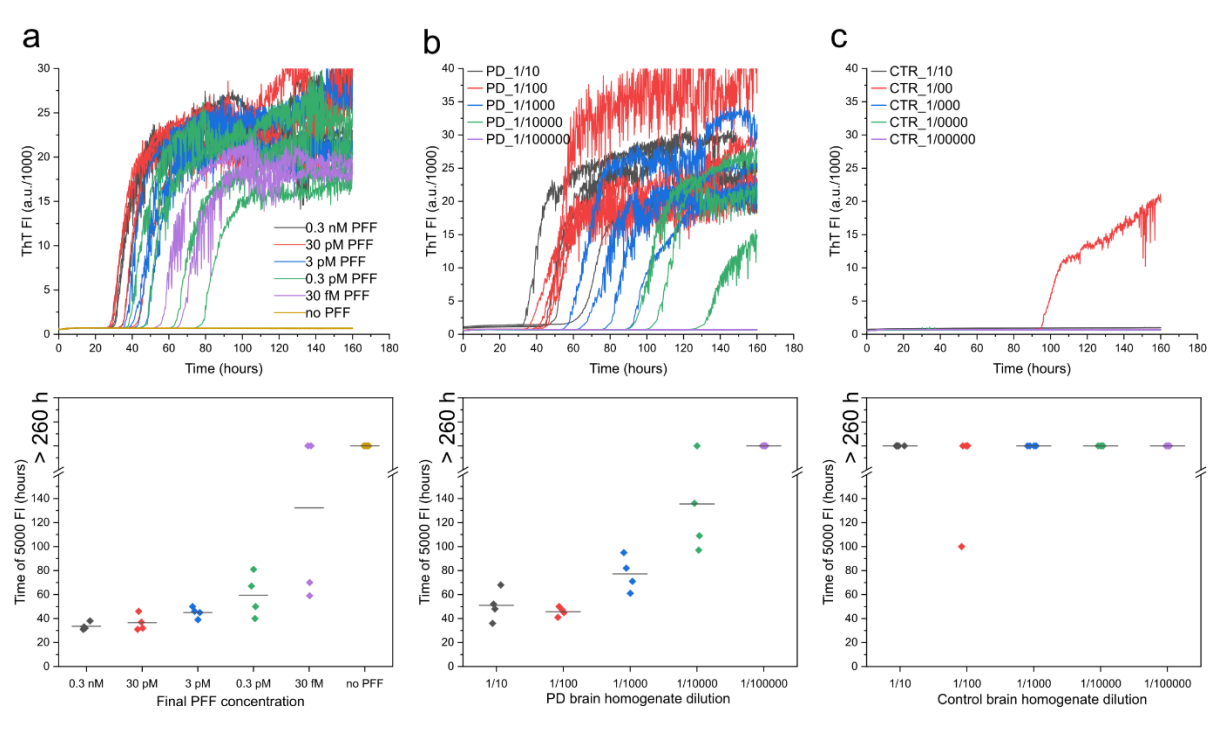

Figure 2: **Quiescent plate-based seed amplification assay (SAA)** using a) pre-formed seeds (PFFs), b) brain extracts from PD patients, and c) brain extracts from healthy controls. Top row: Raw ThT traces. Bottom row: Time at which signal reached 5000 fluorescence units (arbitrary threshold for comparison). The diamonds correspond to the raw data points from 4 repetitions of each condition (top) with mean value indicated by the lines. All experiments were carried out with 10 µM αSyn monomer in the presence of different concentrations of PFFs or brain extract dilutions indicated in the legends.

To imitate the microdroplet conditions (oil droplets stabilized by a PEG-based surfactant) in the conventional plate-based asssay, we used PEG-coated non-binding plates and covered the reaction mixtures in the microwells with a thin layer of fluorinated oil containing the droplet-stabilizing surfactant. Under these conditions, we were able to nearly completely eliminate the false positives of SAAs under quiescent conditions and observed efficient amplification of pre-formed seeds (PFFs) at concentrations down to 30 fM in terms of monomer equivalents (**Figure 2 a**). We analyzed the SAA experiments using the AmyloFit webserver that allows to test different microscopic mechanisms and confirmed that the secondary nucleation increased to levels similar to those of the secondary processes achieved in traditional shaking-based RT-QuIC assays (**Supplementary figure S3**). Before implementing these solution conditions into the microemulsion droplet-based assay, we wanted to test whether they allow to reliably discriminate

between biological samples derived from healthy and PD patients. We performed SAA assay under the same set of conditions in plates without shaking using brain extracts from PD patients (**Figure 2 b**) or healthy individuals (**Figure 2 c**) instead of the PFFs. We found that these assay conditions very robustly discriminate between these two classes of samples. Having established the solution conditions that work in the conventional plate-based assay, we proceeded to implement them into the micro-emulsion droplet platform for the digital assay.

Towards this end, we designed a microfluidic device that allows changing the pH inside the droplet storage chamber. This procedure is advantageous compared to the pre-adjustment of pH, because fibrils tend to stick to the microfluidic tubing and inlet channels or form larger clusters at low pH. We designed dialysis channels next to the storage channel and loaded these with acetic acid that can penetrate through the PDMS from which the devices are fabricated. This decreases the pH of the droplets' content in the main channel to pH ~3, as shown using a pH indicator dye (**Supplementary figure S4**). In these experiments, we replaced the conventionally used ThT with commercially available dye Amytracker (Ebba Biotech AB) due to the strong background fluorescence of ThT as it appeared to partition to some extent into the oil phase surrounding the microemulsion droplets (**Supplementary figure S5**).

First, we loaded the PFFs and the monomer into the droplets and allowed them to elongate for 16 h. After that, the pH was lowered to 3 via dialysis to promote secondary nucleation. Remarkably, we did not observe efficient seed amplification in the droplets after 96 hours under these low-pH conditions, even in seed concentrations as high as 10 nM (**Supplementary figure S6**). We only observed a modest increase in fluorescence intensity in the first 6 hours of the experiment at pH 7.4 that reached a plateau (**Supplementary figure S6, Supplementary video 1**) and remained mostly unchanged even upon shift to lower pH at which increase of ThT signal was observed in the plates. Similar results were obtained when dialysis to pH 3 was performed immediately after droplet formation and even for non-dialyzed droplets kept at neutral pH throughout the experiment (**Supplementary figure S6**). We quantified the concentrations of fibrils inside the droplets after the growth, in order to probe what fraction of the initially added monomer was still available. We calibrated the fluorescence signal intensity by creating a series of droplets that were loaded with different known concentrations of pre-formed fibrils (**Supplementary figure S7**). The result showed that the seed growth ceases after reaching ca. 43 times the mass of the initial seeds, i.e. 0.2, 1, and 5 nM seeds grew to ca 14, 58, and 216 nM fibrils, respectively (all in terms of monomer equivalent concentrations) (**Figure 3 a, b**). The low plateau level that was reached during these experiments showed that not only seed amplification is absent but also that the elongation of fibrils ceases after a few hours, regardless of the conditions. Assuming the initial length of the seeds (ca. 100 nm) and the approximately 40-fold increase in fluorescence, we calculated that the fibrils grew to several micrometers in length before they ceased to grow (**Figure 3 c**). This might be caused by their higher order assembly into clusters that we have previously shown to be length-dependent and strongly enhanced at acidic pH [37]. We also recorded time lapse videos (**Supplementary video 1**) of the droplet-based SAAs where we observe all aggregates inside a given droplet to end up in a single large cluster. This higher order assembly/flocculation probably renders many fibril ends inaccessible to further monomer addition. This conclusion is corroborated by the finding that even an increase in the concentration of monomer does not lead to a higher plateau level of fluorescence above 40 µM (**Supplementary figure S8**).

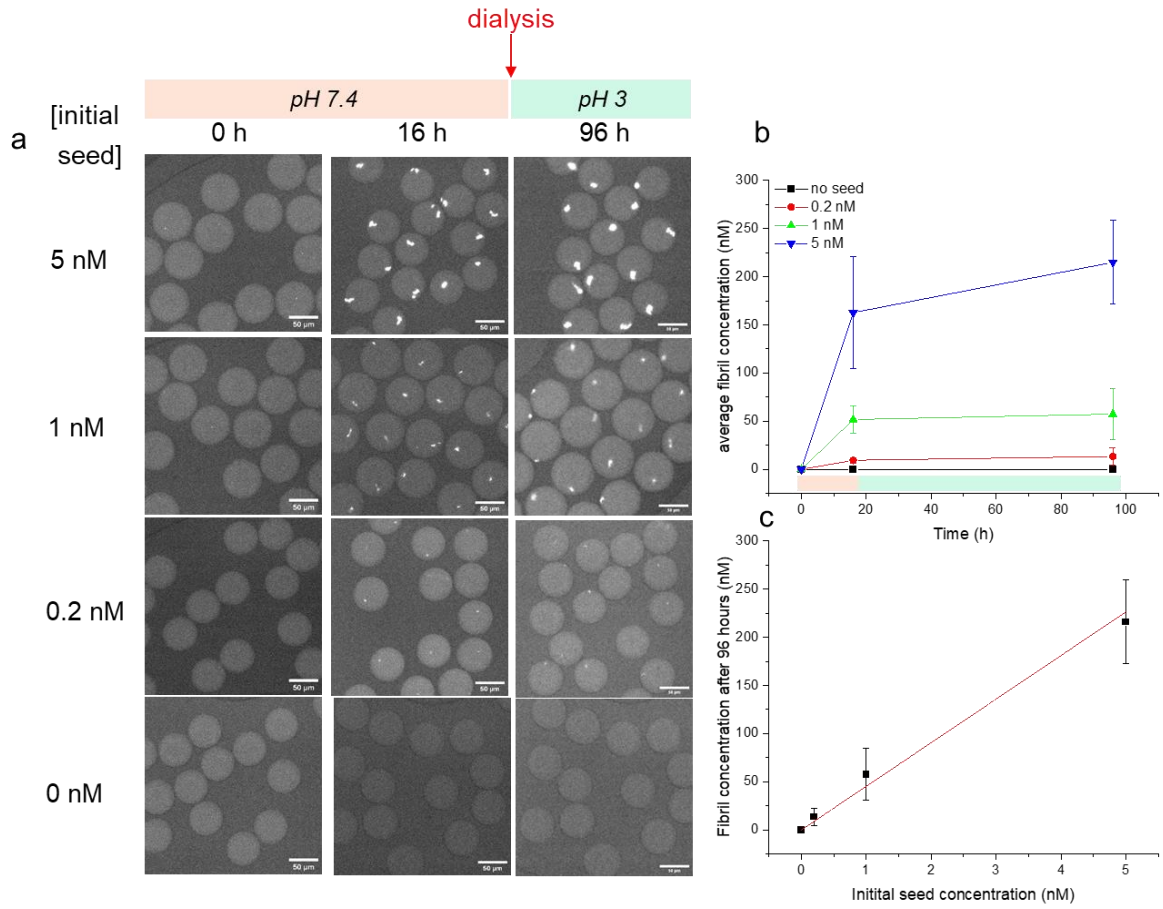

Figure 3: **Implementation of SAA in microemulsion droplets.** a) Fluorescent microscope images of the droplets filled with different concentrations of PFF and 40 μM αSyn monomer in 10 mM NaPi, pH 7.4 and 250 mM sodium sulphate. In the first 16 hours, the droplets were kept in the neutral pH to assure the growth, then the pH was reduced to 3 by loading the dialysis channels with 200 mM acetic acid (pH 3) and the droplets were incubated for an additional 80 hours to monitor the secondary nucleation. b) The kinetic time courses of the same droplets show that fibril growth ceases after the incomplete growth phase. c) the final fluorescence level is directly proportional to the amount of initially added PFFs, suggesting that the seed fibrils grow to ~40 times of their initial length. Droplets were incubated at room temperature.

To elucidate the strikingly different amplification behavior in droplets and microwell plates, we performed parallel experiments under identical conditions in two fluorescence plate readers in which the only difference was the frequency of the reading cycles. By this experiment we wanted to test our hypothesis that even the gentle movement of the plate during measurements could be responsible for the difference compared to the completely quiescent experiments inside the microemulsion droplets. The plate reader moves the plate between measurements in different wells leading to gentle agitation even in the quiescent mode. The effect of plate movements during reading has previously been reported for the aggregation kinetics of amyloid-β [38].

We measured the same aggregation reaction at 10 min (standard condition in our laboratory) and 2 hour reading cycles in parallel using the two identical plate readers (Omega Fluorstar, BMG). The samples in the latter set-up experience at least one order of magnitude less movement than the ones in the measurement with standard cycle duration. Interestingly, the difference in cycle time manifested itself in both the lag

time and final ThT signal intensity; the plate with the shorter cycle time features the shorter lag-time and higher ThT signal of the plateau (**Figure 4 a-c**). In the experiment with 10 minute cycles, the lag-time decreased systematically with increasing concentration of seeds from 1 pM to 20 nM. However, in the experiment with 2h long reading cycles, only 2/4 of the samples with highest seed concentration measured (20 nM) showed sigmoidal increase of fluorescence in the time-course of the experiment (180 hours), whilst no signal was observed for lower seed concentrations (**Figure 4 b**). We also ensured that the observed difference in amplification efficiency truly stems from the different levels of mechanical movement and not from differences in sample heating due to different frequencies of excitation with the light source. To establish this, we conducted two identical assays simultaneously, employing different numbers of flashes of the light source per reading cycle: one cycle with 20 flashes and the other with only one flash per cycle (**supplementary figure S9**). The results of the two assays were very similar, except for the higher signal-to-noise level expected for the cycle with the 20 flashes. This result clearly demonstrates that the absence of active shaking in the plate does not correspond to the complete elimination of impactful mechanical effects during measurement. Based on these results, we hypothesized that the complete absence of seed amplification inside the microemulsion droplets is caused by the absolute quiescence of such experiments.

To test whether some level of mechanical perturbation experienced by the seeds inside the microdroplets would enable seed amplification, we incorporated an oscillating steel sheet in connection with a ferroelectric ceramic piezo chip powered by a circuit board producing a fixed frequency of 108 KHz into the microfluidic device (**Supplementary figure S10**). We visualized the effect of operating the piezo shaker in droplets filled with fluorescent micro particles (**Supplementary movie 2**). We then used this system to probe the effect of mechanically perturbing the droplets on the growth of the fibrils at different pH values (acidic and neutral) and salt concentrations. We saw clear evidence for seed amplification in the samples subjected to mechanical perturbation by ultrasound (**Figure 4 d**). We explored different conditions affecting sonication of the droplets, including a strongly acidic (pH 3) condition aimed at enhancing secondary nucleation, neutral pH with and without sodium sulfate, and high phosphate concentrations. Quiescent droplets containing 0.3 nM PFF exhibited approximately 50-fold increase in their fibril concentration (as seen in Figure 3), whereas the ultrasound-treated droplets yielded final fibril concentrations 1000-fold higher than at the beginning of the experiment. Overall, sonication showed consistent effect across these conditions with the high phosphate environment demonstrating growth and amplification that is slightly more pronounced.

Taken together our results clearly suggest that some level of mechanical agitation, however gentle, is necessary to allow fibrils of αSyn to amplify. The total quiescence inside micro-emulsion droplets is not conducive to fibril amplification, even by secondary nucleation. This conclusion is also consistent with recent results in a study that developed a digital SAA of αSyn in microwells, droplets and microgel particles [28]. In that study, the authors found that 1-2 orders of magnitude lower concentration of particles were detected when the experiments were performed with pre-formed fibrils. This is presumably because under the mildly acidic conditions employed in their study, fibrils tend to cluster together and therefore growing clusters of fibrils were detected, rather than individual fibrils. While the exclusive elongation/growth of the fibrils within a sufficiently large cluster can increase fluorescence intensity to an easily detectable level, this may be more difficult for an individual growing fibril. It would therefore be useful to be able to induce true fibril amplification inside microdroplets through an increase in the number of fibrils rather than only growth from the ends of the initially present fibrils. In the present study, we demonstrate that this can be achieved by subjecting the microemulsion droplet storage device to ultrasonic oscillations.

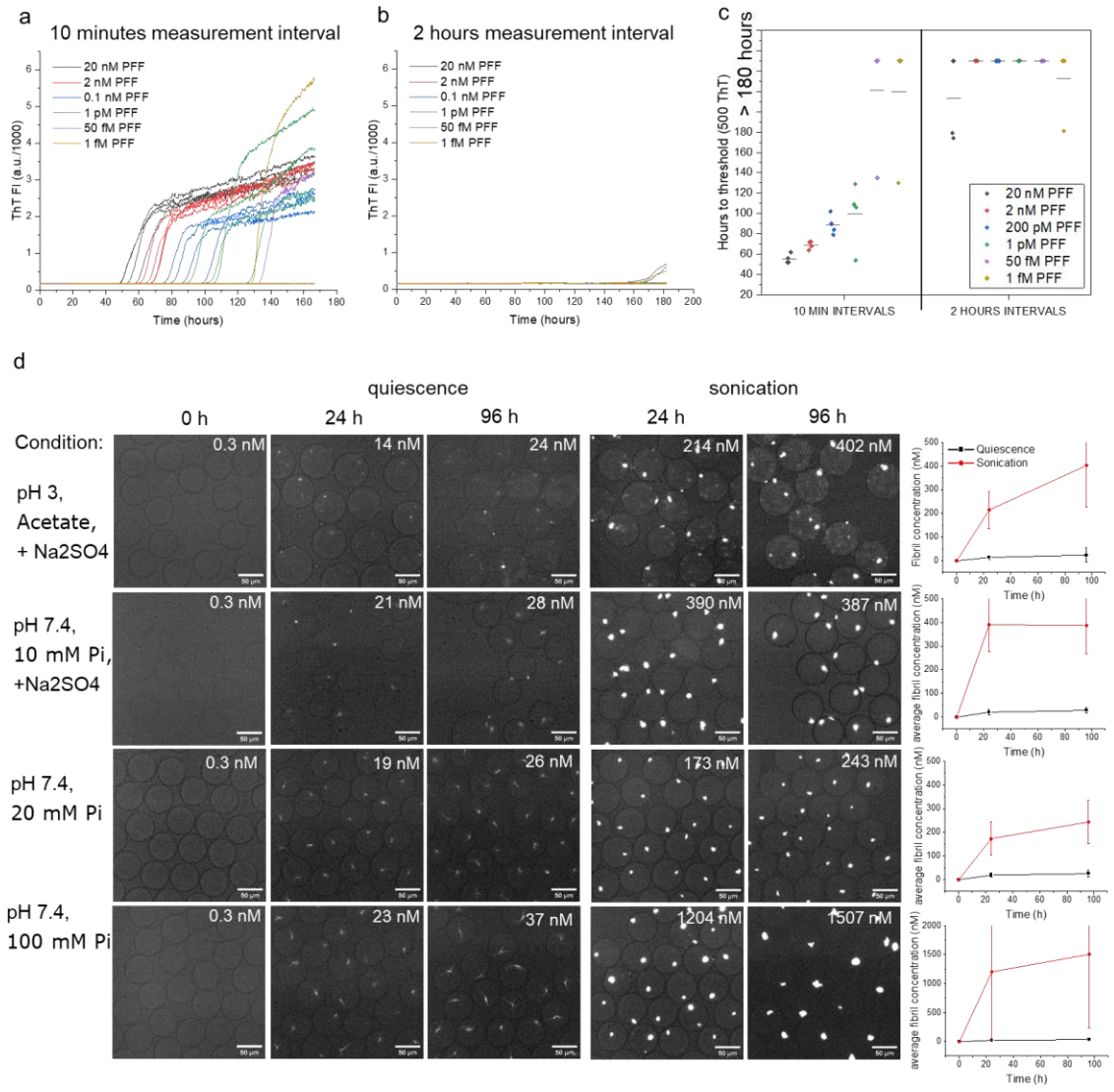

Figure 4: The effect of mechanical perturbations on low-pH SAA in plates (panels a-c) and in microemulsion droplets (panel d). a) Plate-based SAA with 10 min time interval between readings. b) Plate-based SAA with 120 min time interval between readings. c) Analysis of the time until a certain threshold ThT intensity is reached for the two setups shown in a) and b). d) Microdroplet-based SAAs (300 pM PFF) where the droplets are subjected to ultrasound are compared with non-agitated (quiescent) droplets. The different rows show different solution conditions: The first row shows the acidic pH 3 condition similar to that of Figure 3. The other rows show droplet-based SAAs under neutral pH conditions and various ionic strengths. Inset numbers report the concentration of fibrils (as monomer equivalents) at the endpoint of the reaction according to the standard curve. In this figure, Amytracker^{TM} 680 was used to achieve even lower background fluorescence compared to Amytracker^{TM} 480 in Figure 3. Droplets were incubated at 37 ^{0}C. It is noteworthy that it was necessary to cover the droplet storage chamber with a glass coverslip in order to prevent evaporation and droplet shrinkage. This precaution preserves the droplets intact during the 96 hours of experiment (see the supplementary figure S10).

In addition to pointing towards a more efficient manner of designing digital SAAs for alpha-synuclein, we also establish a set of conditions that allows plate-based SAAs to be conducted in the absence of active shaking. Furthermore, we demonstrate that the *de novo* formation of fibrils can be completely suppressed

in plate-based assays by reducing the surfaces catalyzing fibril nucleation using PEGylated plates and covering the solutions with a fluorinated oil containing a PEG-based surfactant.

It is interesting to note that despite the observed enhancement of amplification by the ultrasonic treatment, full conversion of the monomeric substrate inside the microdroplets is not achieved. This contrasts with typical seed amplification assays in plates, where usually complete conversion is achieved. This could be due to the very different physical regimes reigning inside microdroplets compared to multiwell plates. While it is difficult to estimate the effective shear rates in both scenarios, the Reynolds number can be estimated and is found to differ by up to 5 orders of magnitude (**Supplementary results**). This strong difference in fluid dynamic regime might be able to explain in part why seed amplification is so much more efficient in multiwell plate-based SAAs.

Our results therefore also substantially increase our mechanistic understanding of αSyn secondary nucleation. The finding that seed amplification is undetectable under fully quiescent conditions shows that not only fragmentation, but also fibril surface-catalyzed secondary nucleation depend on mechanical perturbations. This is reminiscent of the secondary nucleation of crystals, where attrition of daughter crystals from mother crystals is a major mechanism of secondary nucleation [39-40]. Perhaps even mild mechanical perturbation is sufficient to remove secondary nuclei from their parent fibril surface, enabling more efficient amplification of the number of fibrils.

Taken together, the results of our study will be crucial for the development of efficient and practically implementable digital seed amplification assays for the diagnostics of synucleinopathies.

Conclusion:

In conclusion, we demonstrate that αSyn fibrils can be efficiently amplified under acidic conditions without shaking in a multiwell plate. However, fibril amplification is very strongly suppressed under the conditions of absolute quiescence inside microemulsion droplets. Fibril amplification can be induced inside microdroplets if the latter are subjected to ultrasonic perturbations. Therefore, secondary nucleation of αSyn crucially depends on mechanical perturbations, similarly to fibril fragmentation.

References:

1. Calabresi, P.; Mechelli, A.; Natale, G.; Volpicelli-Daley, L.; Di Lazzaro, G.; Ghiglieri, V., Alpha-synuclein in Parkinson's disease and other synucleinopathies: from overt neurodegeneration back to early synaptic dysfunction. *Cell Death Dis* **2023,** *14* (3), 176.
2. Chopra, A.; Outeiro, T. F., Aggregation and beyond: alpha-synuclein-based biomarkers in synucleinopathies. *Brain* **2024,** *147* (1), 81-90.
3. Choi, M.; Kim, T. K.; Ahn, J.; Lee, J. S.; Jung, B. C.; An, S.; Kim, D.; Lee, M. J.; Mook-Jung, I.; Lee, S. H.; Lee, S. J., Conformation-specific Antibodies Targeting Aggregated Forms of alpha-synuclein Block the Propagation of Synucleinopathy. *Exp Neurobiol* **2022,** *31* (1), 29-41.
4. Goedert, M.; Masuda-Suzukake, M.; Falcon, B., Like prions: the propagation of aggregated tau and alpha-synuclein in neurodegeneration. *Brain* **2017,** *140* (2), 266-278.
5. Chung, H. K.; Ho, H. A.; Perez-Acuna, D.; Lee, S. J., Modeling alpha-Synuclein Propagation with Preformed Fibril Injections. *J Mov Disord* **2019,** *12* (3), 139-151.
6. Parnetti, L.; Gaetani, L.; Eusebi, P.; Paciotti, S.; Hansson, O.; El-Agnaf, O.; Mollenhauer, B.; Blennow, K.; Calabresi, P., CSF and blood biomarkers for Parkinson's disease. *Lancet Neurol* **2019,** *18* (6), 573-586.
7. Rossi, M.; Baiardi, S.; Teunissen, C. E.; Quadalti, C.; van de Beek, M.; Mammana, A.; Stanzani-Maserati, M.; Van der Flier, W. M.; Sambati, L.; Zenesini, C.; Caughey, B.; Capellari, S.; Lemstra, A. W.; Parchi, P., Diagnostic Value of the CSF alpha-Synuclein Real-Time Quaking-Induced Conversion Assay at the Prodromal MCI Stage of Dementia With Lewy Bodies. *Neurology* **2021,** *97* (9), e930-e940.
8. Iranzo, A.; Fairfoul, G.; Ayudhaya, A. C. N.; Serradell, M.; Gelpi, E.; Vilaseca, I.; Sanchez-Valle, R.; Gaig, C.; Santamaria, J.; Tolosa, E.; Riha, R. L.; Green, A. J. E., Detection of alpha-synuclein in CSF by RT-QuIC in patients with isolated rapid-eye-movement sleep behaviour disorder: a longitudinal observational study. *Lancet Neurol* **2021,** *20* (3), 203-212.
9. Siderowf, A.; Concha-Marambio, L.; Lafontant, D. E.; Farris, C. M.; Ma, Y.; Urenia, P. A.; Nguyen, H.; Alcalay, R. N.; Chahine, L. M.; Foroud, T.; Galasko, D.; Kieburtz, K.; Merchant, K.; Mollenhauer, B.; Poston, K. L.; Seibyl, J.; Simuni, T.; Tanner, C. M.; Weintraub, D.; Videnovic, A.; Choi, S. H.; Kurth, R.; Caspell-Garcia, C.; Coffey, C. S.; Frasier, M.; Oliveira, L. M. A.; Hutten, S. J.; Sherer, T.; Marek, K.; Soto, C.; Parkinson's Progression Markers, I., Assessment of heterogeneity among participants in the Parkinson's Progression Markers Initiative cohort using alpha-synuclein seed amplification: a cross-sectional study. *Lancet Neurol* **2023,** *22* (5), 407-417.
10. Concha-Marambio, L.; Farris, C. M.; Holguin, B.; Ma, Y.; Seibyl, J.; Russo, M. J.; Kang, U. J.; Hutten, S. J.; Merchant, K.; Shahnawaz, M.; Soto, C., Seed Amplification Assay to Diagnose Early Parkinson's and Predict Dopaminergic Deficit Progression. *Mov Disord* **2021,** *36* (10), 2444-2446.
11. Russo, M. J.; Orru, C. D.; Concha-Marambio, L.; Giaisi, S.; Groveman, B. R.; Farris, C. M.; Holguin, B.; Hughson, A. G.; LaFontant, D. E.; Caspell-Garcia, C.; Coffey, C. S.; Mollon, J.; Hutten, S. J.; Merchant, K.; Heym, R. G.; Soto, C.; Caughey, B.; Kang, U. J., High diagnostic performance of independent alpha-synuclein seed amplification assays for detection of early Parkinson's disease. *Acta Neuropathol Commun* **2021,** *9* (1), 179.
12. Brown, J. W. P.; Bauer, A.; Polinkovsky, M. E.; Bhumkar, A.; Hunter, D. J. B.; Gaus, K.; Sierecki, E.; Gambin, Y., Single-molecule detection on a portable 3D-printed microscope. *Nat Commun* **2019,** *10* (1), 5662.
13. Bhumkar, A.; Magnan, C.; Lau, D.; Jun, E. S. W.; Dzamko, N.; Gambin, Y.; Sierecki, E., Single-Molecule Counting Coupled to Rapid Amplification Enables Detection of alpha-Synuclein Aggregates in Cerebrospinal Fluid of Parkinson's Disease Patients. *Angew Chem Int Ed Engl* **2021,** *60* (21), 11874-11883.
14. Horrocks, M. H.; Lee, S. F.; Gandhi, S.; Magdalinou, N. K.; Chen, S. W.; Devine, M. J.; Tosatto, L.; Kjaergaard, M.; Beckwith, J. S.; Zetterberg, H.; Iljina, M.; Cremades, N.; Dobson, C. M.; Wood, N. W.; Klenerman, D., Single-Molecule Imaging of Individual Amyloid Protein Aggregates in Human Biofluids. *ACS Chem Neurosci* **2016,** *7* (3), 399-406.
15. Herrmann, Y.; Kulawik, A.; Kuhbach, K.; Hulsemann, M.; Peters, L.; Bujnicki, T.; Kravchenko, K.; Linnartz, C.; Willbold, J.; Zafiu, C.; Bannach, O.; Willbold, D., sFIDA automation yields sub-femtomolar limit of detection for Abeta aggregates in body fluids. *Clin Biochem* **2017,** *50* (4-5), 244-247.
16. Blomeke, L.; Pils, M.; Kraemer-Schulien, V.; Dybala, A.; Schaffrath, A.; Kulawik, A.; Rehn, F.; Cousin, A.; Nischwitz, V.; Willbold, J.; Zack, R.; Tropea, T. F.; Bujnicki, T.; Tamguney, G.; Weintraub, D.; Irwin, D.; Grossman, M.; Wolk, D. A.; Trojanowski, J. Q.; Bannach, O.; Chen-Plotkin, A.; Willbold, D., Quantitative detection of alpha-Synuclein and Tau oligomers and other aggregates by digital single particle counting. *NPJ Parkinsons Dis* **2022,** *8* (1), 68.
17. Soto, C., alpha-Synuclein seed amplification technology for Parkinson's disease and related synucleinopathies. *Trends Biotechnol* **2024**.

18. Frey, B.; Holzinger, D.; Taylor, K.; Ehrnhoefer, D. E.; Striebinger, A.; Biesinger, S.; Gasparini, L.; O'Neill, M. J.; Wegner, F.; Barghorn, S.; Hoglinger, G. U.; Heym, R. G., Tau seed amplification assay reveals relationship between seeding and pathological forms of tau in Alzheimer's disease brain. *Acta Neuropathol Commun* **2023,** *11* (1), 181.
19. Ferreira, N. D. C.; Caughey, B., Proteopathic Seed Amplification Assays for Neurodegenerative Disorders. *Clin Lab Med* **2020,** *40* (3), 257-270.
20. Concha-Marambio, L.; Pritzkow, S.; Shahnawaz, M.; Farris, C. M.; Soto, C., Seed amplification assay for the detection of pathologic alpha-synuclein aggregates in cerebrospinal fluid. *Nat Protoc* **2023,** *18* (4), 1179-1196.
21. Saa, P.; Castilla, J.; Soto, C., Ultra-efficient replication of infectious prions by automated protein misfolding cyclic amplification. *J Biol Chem* **2006,** *281* (46), 35245-52.
22. Meisl, G.; Kirkegaard, J. B.; Arosio, P.; Michaels, T. C.; Vendruscolo, M.; Dobson, C. M.; Linse, S.; Knowles, T. P., Molecular mechanisms of protein aggregation from global fitting of kinetic models. *Nat Protoc* **2016,** *11* (2), 252-72.
23. Zhou, J.; Ruggeri, F. S.; Zimmermann, M. R.; Meisl, G.; Longo, G.; Sekatskii, S. K.; Knowles, T. P. J.; Dietler, G., Effects of sedimentation, microgravity, hydrodynamic mixing and air-water interface on alpha-synuclein amyloid formation. *Chem Sci* **2020,** *11* (14), 3687-3693.
24. Campioni, S.; Carret, G.; Jordens, S.; Nicoud, L.; Mezzenga, R.; Riek, R., The presence of an air-water interface affects formation and elongation of alpha-Synuclein fibrils. *J Am Chem Soc* **2014,** *136* (7), 2866-75.
25. Galvagnion, C.; Buell, A. K.; Meisl, G.; Michaels, T. C.; Vendruscolo, M.; Knowles, T. P.; Dobson, C. M., Lipid vesicles trigger alpha-synuclein aggregation by stimulating primary nucleation. *Nat Chem Biol* **2015,** *11* (3), 229-34.
26. Galvagnion, C.; Brown, J. W.; Ouberai, M. M.; Flagmeier, P.; Vendruscolo, M.; Buell, A. K.; Sparr, E.; Dobson, C. M., Chemical properties of lipids strongly affect the kinetics of the membrane-induced aggregation of alpha-synuclein. *Proc Natl Acad Sci U S A* **2016,** *113* (26), 7065-70.
27. Pfammatter, M.; Andreasen, M.; Meisl, G.; Taylor, C. G.; Adamcik, J.; Bolisetty, S.; Sanchez-Ferrer, A.; Klenerman, D.; Dobson, C. M.; Mezzenga, R.; Knowles, T. P. J.; Aguzzi, A.; Hornemann, S., Absolute Quantification of Amyloid Propagons by Digital Microfluidics. *Anal Chem* **2017,** *89* (22), 12306-12313.
28. Gilboa, T.; Swank, Z.; Thakur, R.; Gould, R. A.; Ooi, K. H.; Norman, M.; Flynn, E. A.; Deveney, B. T.; Chen, A.; Borberg, E.; Kuzkina, A.; Ndayisaba, A.; Khurana, V.; Weitz, D. A.; Walt, D. R., Toward the quantification of alpha-synuclein aggregates with digital seed amplification assays. *Proc Natl Acad Sci U S A* **2024,** *121* (3), e2312031121.
29. Costantini, G.; Budrikis, Z.; Taloni, A.; Buell, A. K.; Zapperi, S.; La Porta, C. A. M., Fluctuations in Protein Aggregation: Design of Preclinical Screening for Early Diagnosis of Neurodegenerative Disease. *Physical Review Applied* **2016,** *6* (3), 034012.
30. Fairfoul, G.; McGuire, L. I.; Pal, S.; Ironside, J. W.; Neumann, J.; Christie, S.; Joachim, C.; Esiri, M.; Evetts, S. G.; Rolinski, M.; Baig, F.; Ruffmann, C.; Wade-Martins, R.; Hu, M. T.; Parkkinen, L.; Green, A. J., Alpha-synuclein RT-QuIC in the CSF of patients with alpha-synucleinopathies. *Ann Clin Transl Neurol* **2016,** *3* (10), 812-818.
31. Shahnawaz, M.; Tokuda, T.; Waragai, M.; Mendez, N.; Ishii, R.; Trenkwalder, C.; Mollenhauer, B.; Soto, C., Development of a Biochemical Diagnosis of Parkinson Disease by Detection of alpha-Synuclein Misfolded Aggregates in Cerebrospinal Fluid. *JAMA Neurol* **2017,** *74* (2), 163-172.
32. Perra, D.; Bongianni, M.; Novi, G.; Janes, F.; Bessi, V.; Capaldi, S.; Sacchetto, L.; Tagliapietra, M.; Schenone, G.; Morbelli, S.; Fiorini, M.; Cattaruzza, T.; Mazzon, G.; Orru, C. D.; Catalan, M.; Polverino, P.; Bernardini, A.; Pellitteri, G.; Valente, M.; Bertolotti, C.; Nacmias, B.; Maggiore, G.; Cavallaro, T.; Manganotti, P.; Gigli, G.; Monaco, S.; Nobili, F.; Zanusso, G., Alpha-synuclein seeds in olfactory mucosa and cerebrospinal fluid of patients with dementia with Lewy bodies. *Brain Commun* **2021,** *3* (2), fcab045.
33. Han, J. Y.; Shin, C.; Choi, Y. P., Preclinical Detection of Alpha-Synuclein Seeding Activity in the Colon of a Transgenic Mouse Model of Synucleinopathy by RT-QuIC. *Viruses* **2021,** *13* (5).
34. Kakuda, K.; Ikenaka, K.; Araki, K.; So, M.; Aguirre, C.; Kajiyama, Y.; Konaka, K.; Noi, K.; Baba, K.; Tsuda, H.; Nagano, S.; Ohmichi, T.; Nagai, Y.; Tokuda, T.; El-Agnaf, O. M. A.; Ogi, H.; Goto, Y.; Mochizuki, H., Ultrasonication-based rapid amplification of alpha-synuclein aggregates in cerebrospinal fluid. *Sci Rep* **2019,** *9* (1), 6001.
35. Jung, B. C.; Lim, Y. J.; Bae, E. J.; Lee, J. S.; Choi, M. S.; Lee, M. K.; Lee, H. J.; Kim, Y. S.; Lee, S. J., Amplification of distinct alpha-synuclein fibril conformers through protein misfolding cyclic amplification. *Exp Mol Med* **2017,** *49* (4), e314.
36. Wang, Z.; Becker, K.; Donadio, V.; Siedlak, S.; Yuan, J.; Rezaee, M.; Incensi, A.; Kuzkina, A.; Orru, C. D.; Tatsuoka, C.; Liguori, R.; Gunzler, S. A.; Caughey, B.; Jimenez-Capdeville, M. E.; Zhu, X.; Doppler, K.; Cui, L.;

Chen, S. G.; Ma, J.; Zou, W. Q., Skin alpha-Synuclein Aggregation Seeding Activity as a Novel Biomarker for Parkinson Disease. *JAMA Neurol* **2020,** *78* (1), 1-11.
37. Buell, A. K.; Galvagnion, C.; Gaspar, R.; Sparr, E.; Vendruscolo, M.; Knowles, T. P.; Linse, S.; Dobson, C. M., Solution conditions determine the relative importance of nucleation and growth processes in alpha-synuclein aggregation. *Proc Natl Acad Sci U S A* **2014,** *111* (21), 7671-6.
38. Sebastiao, M.; Quittot, N.; Bourgault, S., Thioflavin T fluorescence to analyse amyloid formation kinetics: Measurement frequency as a factor explaining irreproducibility. *Anal Biochem* **2017,** *532*, 83-86.
39. Mersmann, A., Attrition and Attrition-Controlled Secondary Nucleation. In *Crystallization Technology Handbook (1st ed.)*, CRC Press. : 2001.
40. Bosetti, L.; Mazzotti, M., Population Balance Modeling of Growth and Secondary Nucleation by Attrition and Ripening. *Crystal Growth & Design* **2020,** *20* (1), 307-319.